ChemPubSoc Europe

DOI: 10.1002/slct.201601532

Chemistry SELECT Full Papers

Catalysis

Ga Modified Zeolite Based Solid Acid Catalyst for Levulinic Acid Production

Vijay Bhooshan Kumar, Indra Neel Pulidindi, Rahul Kumar Mishra, and Aharon Gedanken*[a]

Gallium modified zeolite (mordenite), a solid acid catalyst, was prepared using the sonochemical method. The catalyst (Ga@mordenite) was characterized using XRD, SEM, TEM, EDS, FT-IR, DSC TGA, TPD and XPS analysis. Uniform distribution of Ga on the zeolite surface was confirmed from the SEM-EDS analysis. The catalyst was further used for the production of levulinic acid (LA) from carbohydrates (glucose, starch, and cellulose) in a hydrothermal process. Reaction conditions (time, 6 h; temperature, 175 °C) for the optimum yield of LA (59.9 wt. %) were deduced. The reaction products were analyzed qualitatively using ^{13}C NMR and quantified using HPLC analysis. Synergistic effect of the Lewis acid sites of Ga^{3+} generated in situ and the Bronsted acid sites of mordenite were found to be crucial for the activity of Ga@mordenite for the conversion of glucose to levulinic acid.

1. Introduction

Devising green and sustainable technologies for the conversion of waste biomass to biofuels and biochemicals is a challenge. Limited oil feedstock as well as the accompanied environmental hazards are the key factors motivating the drive towards exploiting alternate feedstock for chemicals production.[1] Protection of the natural environment is of immense significance for building a sustainable and healthy future.[2] Conversion of biomass into useful chemicals is one of the current trends in green chemistry.[3,4] A wide variety of fossil fuel based chemicals for day to day life are produced by industries.[5–7] Biomass rich in cellulose is a sustainable feedstock for the production of fine chemicals and biofuels. Atom efficient, cost-effective and green strategies for the conversion of biomass are sought after.

Glucose is the monomeric sugar obtained upon the hydrolysis of starch/cellulose of the plant materials. A wide range of chemicals are produced on a lab scale using glucose.[8,9] Levulinic acid (LA)[10], γ-valerolactone[11,12] and hydroxy methyl furfural (HMF)[13] are examples of such products. LA is traditionally prepared by treating cellulosic biomass with an acid catalyst. LA could be produced from a wide range of cellulosic feedstock like *Cicer arietinum*, cotton, *Pinus radiata* and sugarcane bagasse.[14]

Currently, there is an increased interest in Ga based materials for catalytic applications.[15–18] Gedanken et al., developed sonochemical strategies for the preparation of GaO(OH)[19], Ga doped carbon dots[20] and polymer dispersed metallic Ga.[21] One of our research interests is to exploit the catalytic properties of Ga for biomass conversion. Carbon based materials (like activated carbon, graphite), silica based materials (like MCM-41) and aluminosilicates (like zeolites) serve as potential support material for the active component Ga. High yields of LA from glucose could be achieved by combining Bronsted and Lewis acid systems.[22] Yang et al., reported strong synergistic catalytic activity of a Lewis ($CrCl_3$) and Bronsted (H_3PO_4) mixed acid system for the conversion of hexose to levulinic acid.[23] Fundamental studies on Ga modified zeolites (H-ZSM-5, Hβ, mordenite, MFI) were reported.[24,25] These reports motivated us to develop a solid acid catalyst with a combination of Bronsted (zeolite mordenite) and Lewis acid sites (Ga species) using a novel sonochemical method and exploit the same for biomass conversion to levulinic acid.

Zeolite mordenite is a synthetic counterpart to the mineral mazzite. The aluminosilicate framework consists of columns of mordenite cages bridged by oxygen atoms to give a 12-membered cylindrical main channel system along the crystallographic c-axis.[26] Previously, heterogeneous acids such as LZY, HY and ZRP–X type-zeolites, metal chlorides and solid super acid ($S_2O^{2-}_8/ZrO_2$-SiO_2-Sm_2O_3) were used to produce LA from fructose, glucose, cellulose and rice straw.[27–30] Jow et al. used molten D-fructose as carbon precursor and LZY zeolite powder as solid acid catalyst for the production of LA and HMF in a sealed batch reactor at 140 °C for 15 h resulting in 44 wt. % conversion of D-fructose to HMF and LA.[31] Chen et al. have examined the production of LA from rice straw using a solid super acid ($S_2O^{2-}_8/ZrO_2$-SiO_2-Sm_2O_3) and reported a LA yield of 22.8 wt. %.[28] Ya'aini et al., have synthesized hybrid catalysts ($CrCl_3$ and HY zeolite) and used the same for the conversion of glucose to LA with a conversion value of 62 wt. % (160 °C, 3 h).[30] Highly reactive acid sites were found to influence the conversion of glucose to levulinic acid. Moreover, enhanced LA yields were obtained in short reaction times, and at high

[a] *V. B. Kumar, I. N. Pulidindi, R. K. Mishra, A. Gedanken*
Bar Ilan Institute for Nanotechnology and Advanced Materials, Department of Chemistry
Bar-Ilan University
Ramat-Gan 52900, Israel
Tel: +972 3 5318315
Fax: +972 3 7384053
E-mail: gedanken@mail.biu.ac.il

Supporting information for this article is available on the WWW under http://dx.doi.org/10.1002/slct.201601532

Table 1. Production of LA from biomass using zeolite based catalysts

Feedstock	Reaction conditions	Catalyst	Yield/ Conversion (wt. %)	Reference
Glucose	Hydrothermal reaction in N_2 environment; 400 rpm; 1.7 Mpa; 8 h; 180 °C; Catalyt preactivation at 550 °C for 4 h; Glucose:catalyst (w/w) = 1.33; Catalyst reusability is not tested;	MFI type zeolites	Yield - 35	[35]
Glucose	Pressure reactor; 180 °C; 200 rpm; 3 h; Glucose:catalyst (w/w) = 1:1; Reusability of the catalyst tested for five successive cycles; Catalyst regenerated by calcination at 400 °C for 5 h; Decrease in LA yield is less than 15% after five reaction cycles:	10 wt. % Fe/ HY zeolite	Yield - 62	[36]
Furfuryl alcohol	Furfuryl alcohol (1 M); THF/H_2O w/w = 1:2; Furfuryl alcohol: Catalyst (w/w) = 0.6; 120 °C, 700 rpm; Catalyst regenerated by calcination at 550 °C for 5 h; Reusability of the catalyst is demonstrated for 4 reaction cycles	H-ZSM-5	Yield - 70	[37]
Xylose	Stainless steel reactor; Hot-compressed water; 170 °C; 15 bar (N_2); Xylose:catalyst = 1.8; reusability of the catalyst not tested	Alkali treated zeolite-Y	Yield - 30 Conversion - 84.2	[38]
Glucose or starch	Hydrothermal reaction; 175 °C; 6 h; Catalyst is reusable for 4 reaction cycles	Ga@mordenite	Yield - 59.9	Current study

reaction temperatures (> 160 °C). Recently, Wang et al. have synthesized zeolite supported metal nanoparticles via base-assisted chemo selective interaction between the silicon species on the zeolite crystal surface and metal salts. The synthesized Ni/ZSM-5 catalyst was used for biomass conversion (hydro deoxygenation of stearic acid to n-alkanes)[32]. There are few reports on the synthesis of Ga-zeolite catalysts, like Ga–H-ZSM zeolite[33], Ga-containing zeolite[25] and isomorphous substitution of Ga in zeolite[34] for the production of fine chemicals. Some of the recent reports on the production of LA using zeolite based catalysts are summarized in Table 1.

From the above reports, it is understood that zeolites form an inexpensive and promising support material for the active metal nanoparticles in the generation of acidic sites that facilitate the conversion of carbohydrates to levulinic acid. There have been almost no reports on the utilization of Ga-zeolite composite catalysts for biomass conversion. Table 1 shows that in several instances, Al was replaced by Ga atom or ion. We report for the first time, a new sonochemical technique for the synthesis of Ga@mordenite NPs. A unique sonochemical approach was employed for designing the Ga-mordenite zeolite catalyst which was subsequently used for the conversion of biomass to LA under hydrothermal reaction conditions. We have recently developed a methodology of sonochemical irradiation of molten metal yielding a variety of new products.[39,40] This method was used for the preparation of Ga@mordenite catalyst. In addition, the current study presents a detailed investigation of the optimized production of LA using the solid acid catalyst in a hydrothermal reaction. The objective of the current work is to develop a viable process for the conversion of carbohydrates to LA under mild reaction conditions.

2. Results and Discussion

2.1. Characterization of Ga@mordenite catalyst

The X-ray diffraction pattern of Ga@mordenite and mordenite (activated) were similar (Figure 1 **(A)).** Intense signals were obtained in the case of activated mordenite. Upon deposition of Ga on mordenite (Ga@mordenite system), a decrease in the intensity of the peaks was noticed (Figure 1(A)).

Moreover, the diffraction peaks typical of gallium particles were not observed owing to the amorphous deposition of gallium particles on zeolite surface. A comparison of the XRD pattern of Ga@mordenite catalyst before and after the hydrothermal reaction was shown in Figure 1(B). Retention of the original crystal structure of the catalyst even after the hydrothermal reaction is inferred from the similar XRD pattern of the catalyst before and after the catalytic reaction (Figure 1 (B)).

TEM and HRTEM images of mordenite alone (after thermal activation) were shown in Figure 2 (A) and Figure 2 (B), respectively. Straight cylindrical pores (fine channels) in the zeolite mordenite perpendicular to the viewing axis could be observed which are analogous to those present in the case of ordered mesoporous silica MCM-41 **(**Figure 2 **(B)).**[41] Small particles of Ga metal (20-70 nm) were observed in Figure 2 **(C)**, which were amorphous in nature. Selected area electron diffraction pattern of the Ga@mordenite particles showed ring pattern typical of the polycrystalline nature of zeolite. The arrows in Figure 2 **(C)** and Figure 2 **(D)** show Ga particles on the surface of mordenite. Small black dot-like features on mordenite could be viewed in Figure 2 **(D)** which could be clusters composed of a few atoms of Ga.

It is worth mentioning that no electron diffraction pattern typical of Ga species (Ga, Ga_2O_3, GaO(OH)) was observed, which is in agreement with the XRD analysis indicating the presence of Ga in amorphous metallic form.

To determine the purity, composition and elemental distribution of Ga in Ga@mordenite material, energy dispersive X-ray spectroscopy (EDS) and elemental mapping were carried

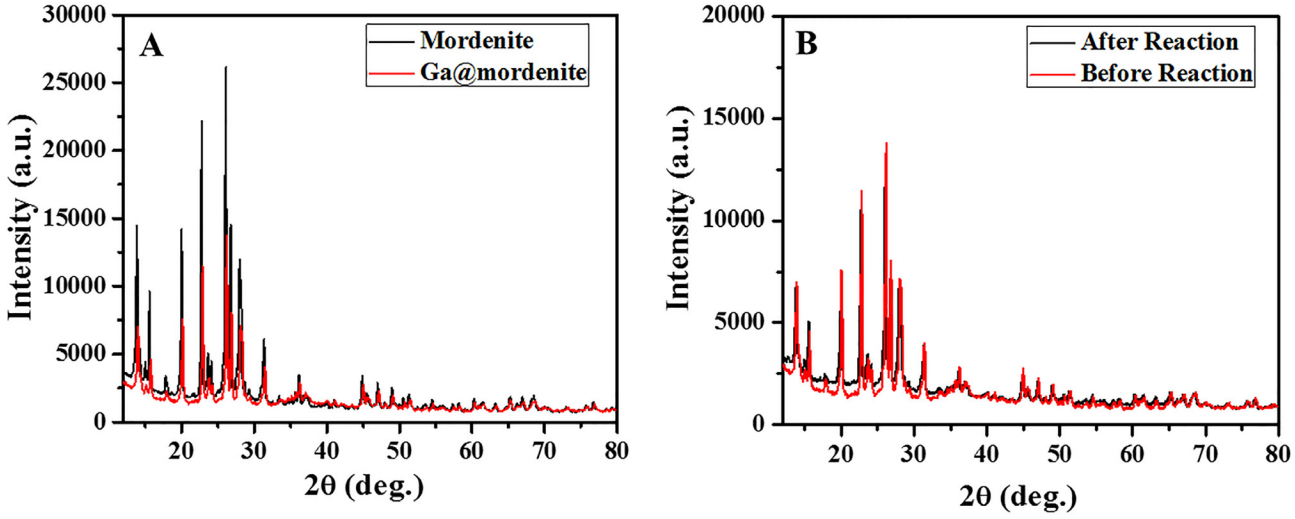

Figure 1. XRD pattern of (A) Ga@mordenite and mordenite alone, (B) Ga@mordenite before and after the reaction..

out. EDS analysis of a sample of the Ga@mordenite catalyst showed the presence of four elements namely, Ga, Al, Si, and O). In accordance with the HR-TEM analysis, clusters of Ga could be observed on the mordenite surface via the Ga mapping (Figure 3). Thus the deposition of Ga on zeolite was proved.

The valence states and the nature of the elements present on the surface of the Ga@mordenite particles were investigated by XPS analysis. Figure 4**a and 4b** show the XPS survey scans of Ga mordenite before and after the reaction.

These two spectra are almost similar giving further evidence of stability of the catalyst. The characteristic peaks corresponding to O 1 s (532.900 eV), Ga 2p (1118.612 eV), Si 2p (103.550) and Al (74.850 eV), and Ga 3d (20.290 eV) were observed in the XPS scan spectrum. In detail, a strong single peak for Ga 2p at 1118.612 eV, and 3d at 20.290 eV were assigned to Ga^{3+}. [20] XPS will give only the surface properties of materials (less than 3 nm depth from the surface). The surface of Ga particles might be covered with Ga_2O_3 or GaO(OH) in the form of Ga^{+3}, but the amount was very low (less than 0.1 %).

The deposition (%) of the Ga particles on mordenite was determined in the following manner: a 12 mg sample of Ga@mordenite was immersed in 0.5 M HNO_3 for about 1 hour to dissolve the particles. Three cycles of evaporation and addition of water were done to dilute the acid, and the final volume of the solution was brought to 10 mL The concentration of Ga was determined by ICP-OES to be 107.7 mg/L. So the total weight of Ga in the sample was 1.07 mg. This corresponds to ca. 8.71 wt % loading of Ga on mordenite. In addition, ICP analysis was carried out on the used catalyst. We have found that the same Ga concentration (~103 mg/L) in Ga@mordenite. Moreover, the leaching of Ga during the reaction into the hydrolysate was tested and found to be very low (concentration of Ga, 8.3 ppm).

Typical TPD profiles of zeolite mordenite and Ga modified mordenite were shown in Figure 5. Two NH_3-desorption peaks centered at 223 and 553 °C were observed in the case of Ga@mordenite which were characteristic of weak (292 μmol/g) and strong (480 μmol/g) acid sites. Upon deposition of Ga on mordenite support, the two afore mentioned NH_3-desorption peaks shifted to higher temperatures, namely, from 178 to 223 °C and 476 to 553 °C respectively. This indicate an increase in the acid strength of the Ga modifeid mordenite for fast and selective prodcuiton of LA production from biomass.

Not only the acid strength but also the quantity of the acid sites, represented by the amount of ammonia desorbed at a particular temperature (μmol/g), was increased in the case of Ga@mordenite relative to mordenite as evident from the data summarized in Table 2.

Table 2. Amount of NH_3 desorbed from mordenite and Ga@mordenite from TPD profiles

Sample	Amount of NH_3-desorbed (μmol/g)		
	Total	Weak acid sties	Strong acid sites
Ga@mordenite	772.4	292.1	480.3
Mordenite	666.3	178.7	487.6

(a) The pore size distribution and the N_2 adsorption-desorption isotherms of mordenite and Ga@mordenite were shown in Figure S1. As expected, the pore size is < 2 nm which is typical of microporous materials. The pore size distribution Ga@mordenite was calculated using Density Functional Theory (DFT).[42] The specific surface area values of mordenite and Ga@mordenite were 421 ± 24 and 348 ± 21 m^2/g, respectively. No significant reduction in the specific surface area value of the mordenite upon Ga deposition is observed as Ga particles were present on the outer surface of the zeolite and not in micropores. Ga particles could not enter the pores because the size of most of the particles was larger than 2 nm.

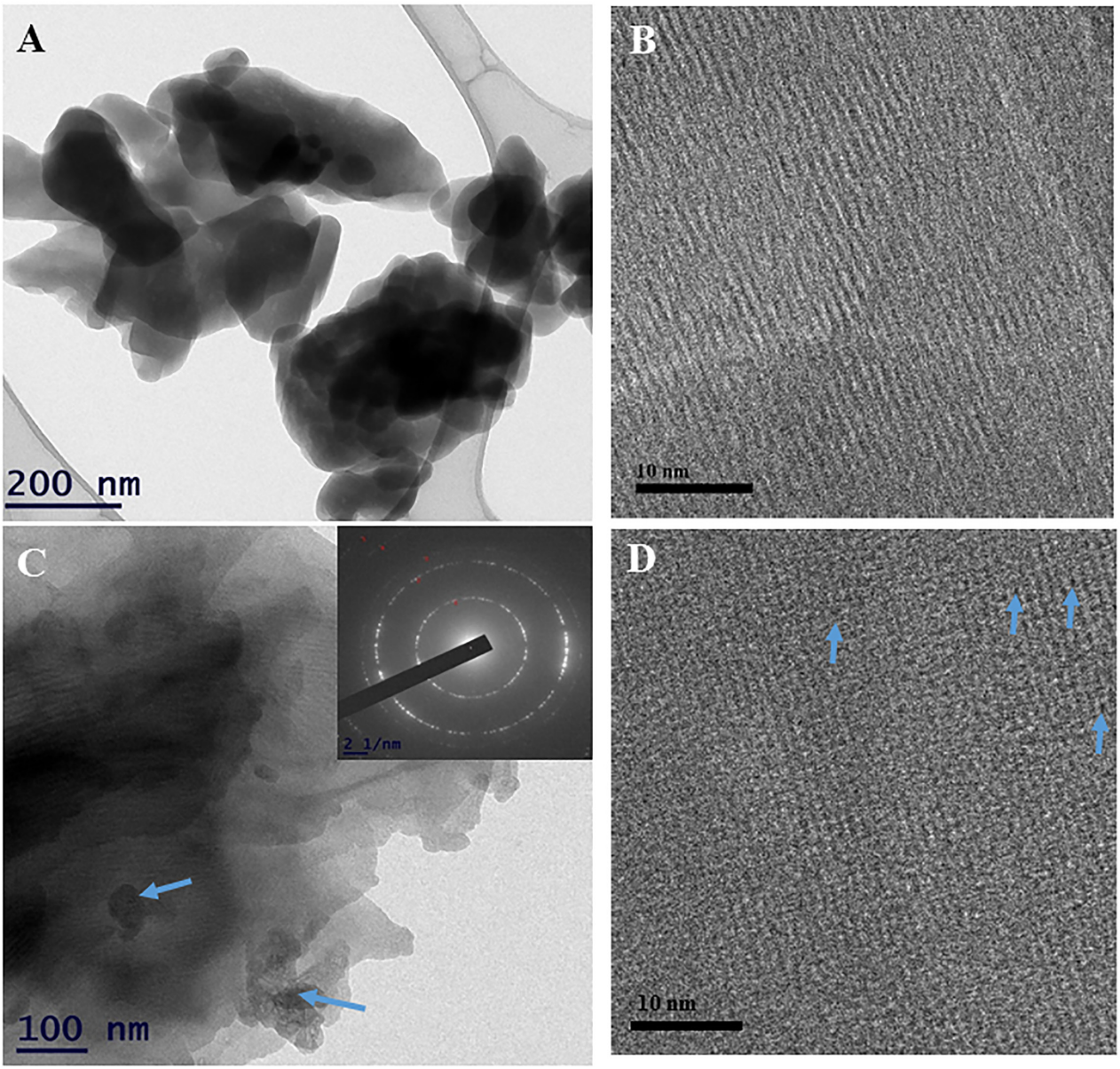

Figure 2. (A) TEM (B) HRTEM images of mordenite alone (after activation) (C) TEM image of Ga@mordenite (inset: selected area electron diffraction) (D) HRTEM image of Ga@mordenite, (arrow mark indicate Ga particles on the surface of mordenite).

(b) The structural stability of mordenite upon Ga deposition under sonochemical conditions was probed using FT-IR spectroscopy (Figure S2). Characteristic peaks were observed at 1120 cm^{-1} (Al-Si–O stretching), 1556 cm^{-1} (Si–O stretching vibration) which are typical of mordenite aluminosilicate. Similar peak pattern was observed in the FT-IR spectrum of Ga@mordenite indicating the structural integrity of mordenite even after sonication for 2 h.

(c) DSC analysis was performed on Ga@mordenite to find the phase of gallium. During the heating, a small endothermic peak appeared at 25.5 °C (Figure S3 A) which is due to the melting of Ga particles present on the surface of mordenite. However, the melting point of Ga is at 29.8 °C and this shift of the melting point to lower temperatures might originate from the small size of Ga particles. Another speculative interpretation is argues that the small endothermic peak is perhaps a super position of two peaks. The first is the endothermic transition due to the Ga melting while the second is an exothermic peak assigned to the amorphous to crystalline transition. The energy of this phase transition is smaller than the melting energy, therefore the endothermic peak is prevailing, while the transition temperature of the amorphous to crystalline is

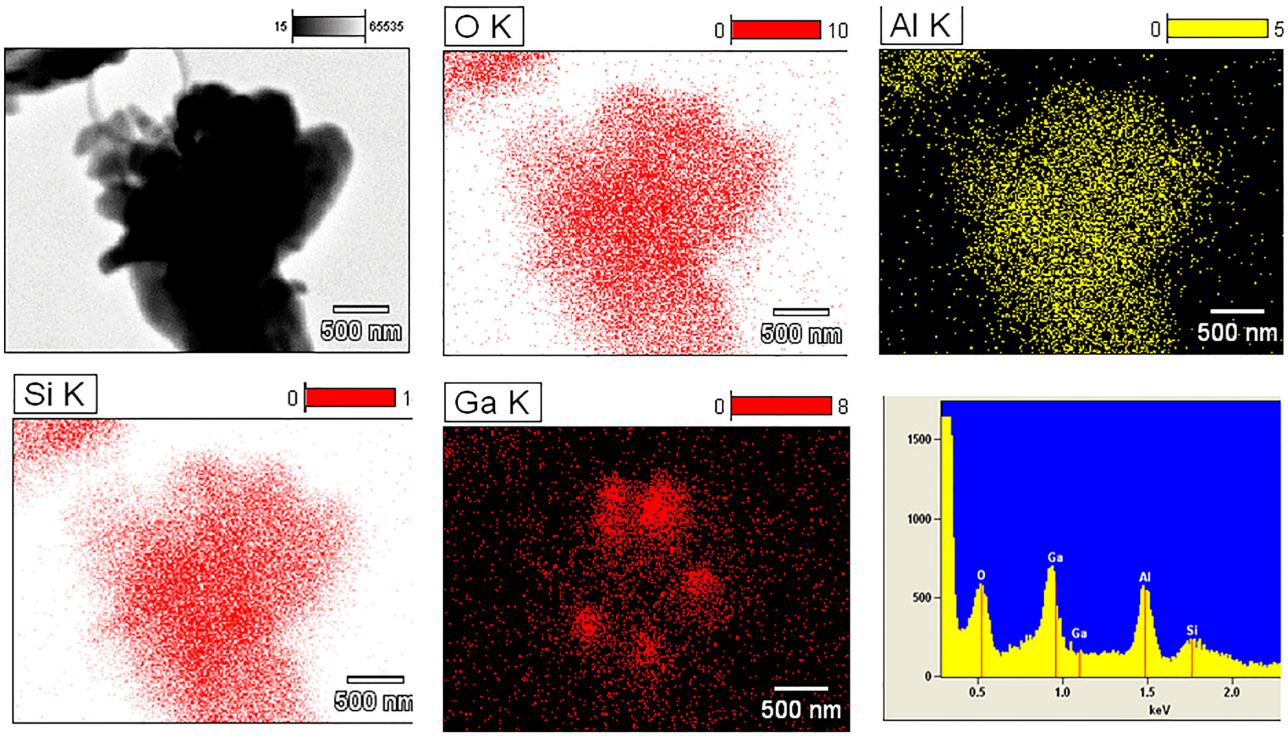

Figure 3. TEM image with the elemental mapping and EDS of Ga@mordenite.

lower than 29.8 °C shifting the endothermic resultant to a lower temperature.

(d) It is well known that the surface of Ga up to a few nm is readily oxidised to either Ga_2O_3 or GaO(OH) and that is why in the case of Ga@mordenite, the XPS spectrum showed Ga^{+3} but the % of oxidation is very low (< 0.1 %).[40] On the contrary, there is no evidence in the XRD plot of Ga@mordenite for the existence of Ga_2O_3 or GaO(OH), indicating that the amount of the oxidized Ga is below the detection limit, and Ga is present in the amorphous phase as Ga^0 (No Ga diffraction peaks observed in Figure 1). TEM and elemental mapping were performed to probe further into the particle distribution and elemental composition of Ga@mordenite, TEM and elemental mapping displayed a uniform distribution of Ga particles on zeolite surface. It is still enticing to probe further into the properties of the surface species on Ga@mordenite. To evaluate the thermal stability of synthesized catalyst thermogravimetric analysis (TGA) was carried out. No significant weight loss indicative of the degradation of Ga@mordenite was observed up to 500 °C (Figure S3 (B)). This indicates, the thermal stability and usefulness of the catalyst, Ga@mordenite under the reaction conditions. On the other hand, it substantiated our interpretation that the DSC in the 20–40 °C does not involve any chemical reaction but rather melting and phase transition processes.

2.2 LA production from carbohydrates

2.2.1 Activity of Ga@mordenite catalyst for LA production from glucose

Hydrothermal reaction of aq. glucose solution (0.5 g in 20 mL) was carried out for 6 h at 120 °C under four different reaction conditions, namely, without catalyst, with gallium alone, with mordenite alone and with Ga@mordenite. The products obtained in each of the four cases were analyzed by ^{13}C NMR and are shown in (Figure 6).

When gallium alone (Figure 6(b)) or mordenite alone (Figure 6(c)) were used as catalyst, the peaks typical of glucose (60.3 (C6), 69.2 (C4), 72.4 (C2), 73.7 (C3), 75.3 (C5), 92 (C1α) and 95.3 (C1β)) (Figure 6(a)) were almost unaltered. In sharp contrast, when Ga@mordenite is used as catalyst, the peaks typical of glucose in the range of 60–100 ppm disappeared completely. In addition, new peaks typical of LA (27.9 (C1), 29.1 (C2), 37.7 (C3) and 177.4 (C4) ppm), lactic acid (La. A) (20, 66, 180 ppm) and formic acid (167 ppm) are detected. This shows the potential of Ga@mordenite catalyst for the complete conversion of glucose. Further studies, were carried out towards optimizing the reaction conditions for the selective conversion of glucose to LA using Ga@mordenite catalyst.

2.2.2. Effect of hydrothermal reaction time on the conversion of glucose:

So as to evaluate the minimum time required for the complete conversion of glucose, the reaction (0.5 g glucose, 0.1 g catalyst

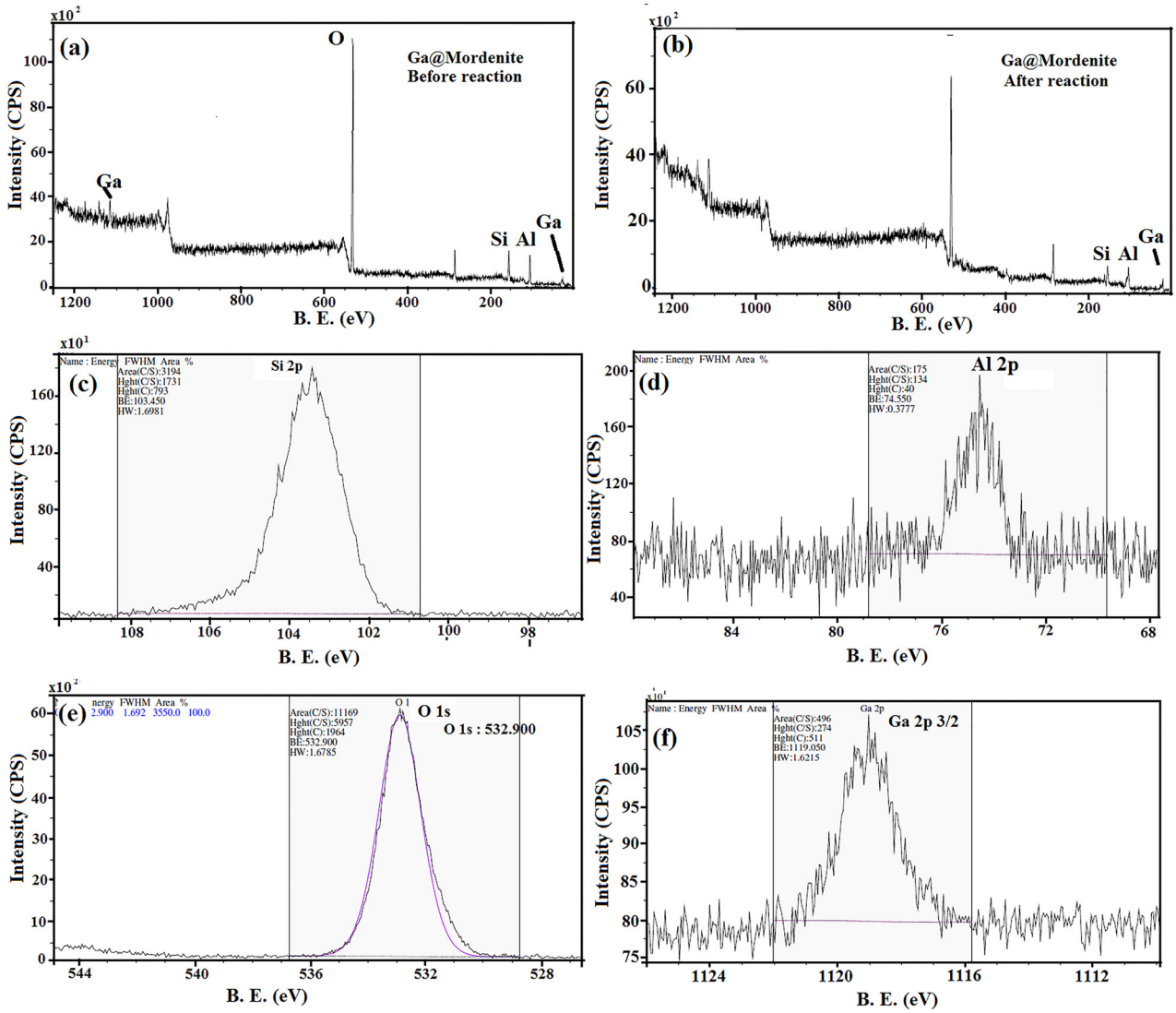

Figure 4. Full XPS spectrum of Ga@mordenite (a) before reaction (b) after reaction (c) XPS spectrum of Si 2p, (d) XPS spectrum of Al 2p (e) XPS spectrum of O 1 s (f) XPS spectrum of Ga 2p..

and 15 mL of DDW in a hydrothermal reactor at 175 °C) was carried out for different periods of time (3, 6, and 9 h). The ^{13}C NMR spectra of the reaction products obtained in each instance were shown in Figure S4. After 3 h of hydrothermal reaction, the signals typical of the reactant glucose (8 consecutive lines in the range of 60–100 ppm) could be still seen indicating that the reaction is not complete (Fig S4 (a)). In the product obtained after 6 h of hydrothermal reaction, the signals due to glucose disappeared completely and signals characteristic of the reaction products (levulinic acid, formic acid and lactic acid) were observed (Figure S4 (b)). The yields of levulinic acid, formic acid and lactic acid determined from HPLC analysis were 59.9, 9.0 and 3.9 wt. %, respectively. Similar features were observed in the case of the reaction product obtained after 9 h of hydrothermal reaction (Figure S4 (c)). Thus 6 h of hydrothermal reaction is the optimal duration required for the complete conversion of glucose to reaction products using Ga@mordenite solid acid catalyst at 175 °C.

2.3. Reusability of Ga@mordenite solid acid catalyst

The reusability of the Ga@mordenite solid acid catalyst was tested for four reaction runs under optimal reaction conditions (175 °C, 6 h). To reduce the loss of catalyst during separation and drying, the reaction product obtained in each case is separated from the catalyst by centrifugation. The regenerated catalyst, Ga@mordenite was transferred into the hydrothermal reactor and the reusability of the catalyst is evaluated. The yield of reaction products and the unreacted glucose (if any), obtained in each of the four successive reaction runs is shown in Figure 7. The LA yield in the first reaction run is 59.9 wt.%. There is no appreciable loss in activity even after five reaction runs. In each reaction run the LA yield is above 58 wt. % as

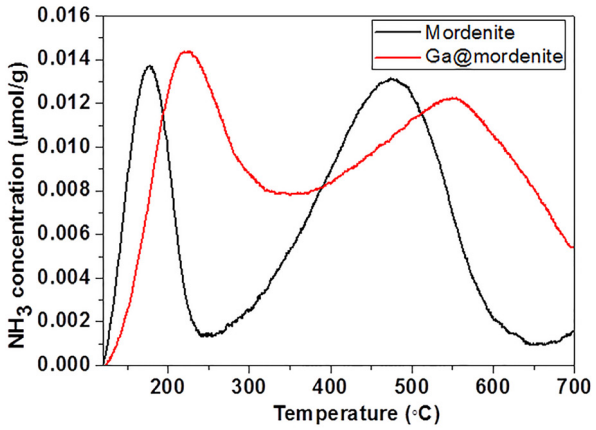

Figure 5. NH_3-TPD profiles of mordenite and Ga@mordenite.

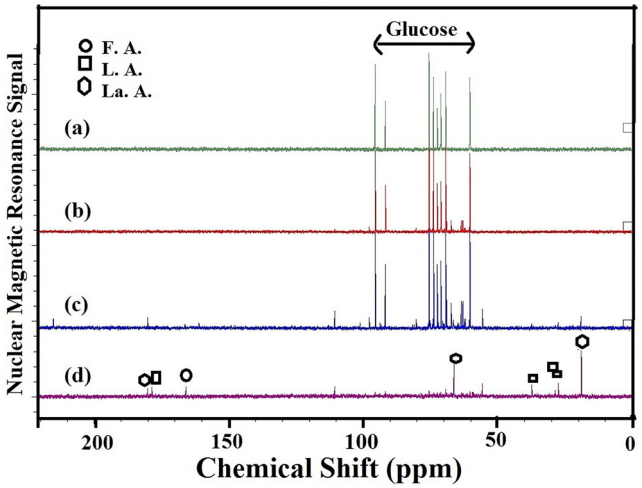

Figure 6. ^{13}C NMR spectra of the product obtained from hydrothermal reaction (6 h; 120 °C) of glucose (a) in the absence of catalyst (neither Ga nor zeolite) (b) with Ga alone (c) with mordenite alone (d) with Ga@mordenite..

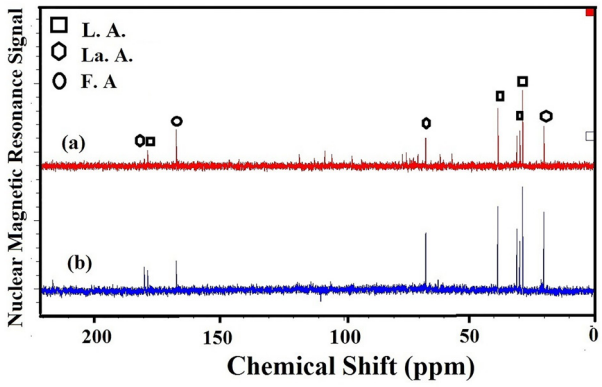

Figure 7. Reusability of Ga@mordenite catalyst for the production of levulinic acid from glucose, (L.A. = Levulinic acid, F.A. = formic acid, and La. A. = lactic acid).

deduced from HPLC. It should be noted that the maximum theoretical yield (wt.%) of LA from glucose as feedstock is 64.4 wt.% .[14] The value of LA yield (~ 60 wt.%) we achieved is not far from the theoretical maximum that could be obtained. The LA yield (~ 60 wt.%) obtained using the heterogeneous catalyst, Ga@mordenite, is comparable to the state of the art catalyst (10 wt. % Fe/HY zeolite, LA yield - 62 wt.%) reported by Ramli et al., 2015.[36] Moreover, Ga@mordenite has the specific advantage of ease of reusability without any high temperature activation in between the reaction runs as required for the catalyst reported by Ramli et al., 2015.[36]

The yield of LA (70 wt.%) reported by Mellmer et al., 2015 (Table 1) using H-ZSM-5 is indeed much higher than the value we currently report.[37] But, it should be noted that Mellmer et al., achieved this yield of LA from furfuryl alcohol as starting material and not glucose as the feedstock. In the case of furfuryl alcohol as the feedstock, the theoretical maximum yield of LA is 118.3 wt.%. Moreover, conversion of furfuryl alcohol to LA is a simple hydrolysis reaction unlike the conversion of glucose to LA which comprises of several reactions, namely, isomerization of glucose to fructose followed by dehydration of fructose to HMF and subsequent rehydration of HMF to levulinic and formic acids.[14,37] Mellmer et al., achieved only 70 wt.% eventhough there is scope for attaining a a much higher yield for LA, i.e. 118.3 wt.% from furfuryl alcohol. Owing to these salient aspects, based on the yield of LA and the stability and reusability of the catalyst, Ga@mordenite is a superior system for the conversion of glucose to LA.

Industrial adoptability of Ga@mordenite catalyst is feasible for the large scale production of levulinic acid, as mordenite has already been demonstrated as a potential industrial catalyst for reactions such as isomerization of alkenes and aromatics.[43] Constrains associated with the microporosity and dimentionality of the mordenite structure could be tuned to mesopore structure when used for reaction such as biomass pyrolysis and cracking of vacuum gas oil.[44]

2.4. Use of starch and cellulose as feedstock for LA production:

The developed methodology for the catalytic conversion of glucose to LA using the solid acid catalyst was further extended to other carbohydrate feedstock such as starch, and cellulose. The ^{13}C NMR spectra of the reaction products obtained from carbohydrate feedstock (starch and cellulose), upon subjecting the same for hydrothermal reaction under the optimal conditions (175 °C, 6 h) were shown in Figure 8.

It is interesting to note that signals typical of the reactant starch were not observed in the hydrolysate. Rather, similar reaction products as obtained in the case of glucose conversion, namely levulinic acid, lactic acid and formic acid were observed (Figure 8(a)). Cellulose too was completely converted to the reaction products (levulinic acid, lactic acid and formic acid) (Figure 8(b)). Signals typical of the intermediate hydrolysis product glucose was not observed in the expected region of 60–100 ppm indicating that the cellulose is completely converted to the reaction products. This indicates the potential of

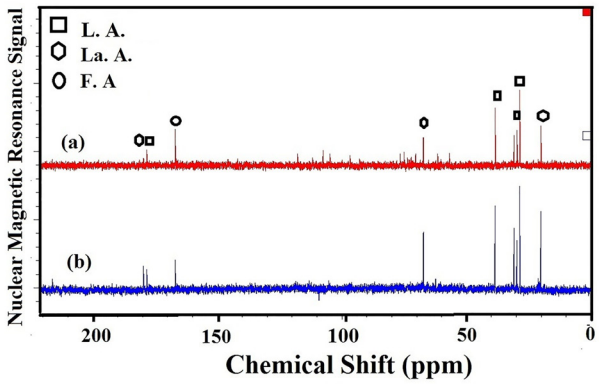

Figure 8. ^{13}C NMR spectra of the product obtained from 6 h hydrothermal reaction at 175 °C of (a) starch, (0.5 g), (b) cellulose (0.5 g), with Ga@mordenite (0.1 g) as catalysts. (LA=Levulinic acid, FA = formic acid, and La. A = lactic acid)

the Ga@mordenite solid acid catalyst for the production of LA from complex biopolymers like cellulose. The yield of LA from the starch and cellulose was 46 and 49 wt. %, respectively.

2.5. Significance of Bronsted and Lewis acidity of Ga@mordenite catalyst for LA production:

Mordenite is a potential Bronsted acid and the bridging hydroxyl between the Si and Al is the acidic site. Isomorphous substitution of Ga in the place of Al in the aluminosilica lattice is known to decrease the Bronsted acidity. As the purpose of the current study is to develop a potential solid acid catalyst for LA production from carbohydrates, it was intended not to isomorphously substitute Al^{3+} by Ga^{3+}, but rather to deposit Ga particles on the surface of mordenite. Such a strategy of using the zeolite as support for Ga has two advantages. The acidity of the support zeolite is retained. The retention of the acidity of the parent zeolite could be envisaged from the retention of the broad band 3630 cm^{-1} which is typical of the bridging hydroxyl between the Al^{3+} and Si^{4+} sites in the mordenite even after Ga deposition (Figure S5).[34] In addition, the Ga particles deposited on the zeolite surface would adopt oxidation state of 3+ in aqueous solution and act as hard Lewis sites during the catalytic transformation of glucose to levulinic acid.[45] It should be noted that Lewis acid sites are vital for bringing about the transformation of glucose to fructose which is the prime reaction in the conversion of glucose to levulinic acid. The fructose, glucose isomerization product, would undergo dehydration to hydroxy methyl furfural and subsequent rehydration to LA through the catalytic function of the Bronsted acid sites of mordenite.[22] Thus the synergistic action of the Lewis acidity of Ga^{3+} and the Bronsted acidity of mordenite result in the potential catalytic activity of the solid acid catalyst for LA production. Possibly the Ga^{3+} ions on mordenite surface could appear as GaO(OH). To evaluate the exact role of Ga^{3+} in the conversion of glucose, Ga_2O_3 is prepared and is reacted under identical reaction conditions. Glucose was found to be selectively converted to HMF. This further confirms the proposed function of Ga^{3+} in the isomerization of glucose to fructose and the subsequent conversion of fructose to HMF. No further conversion of HMF to LA is observed with Ga_2O_3 catalysts possesing only Ga^{3+} sites. For further conversion of HMF to levulinic acid, Bronsted acid sites are required and in the current case mordeinte provides scch acid sites. This justifies the choice of a combination of Ga and mordenite for the catalytic conversion of glucose to levulinic acid. The Lewis acidity of gallium halides[46] and gallium triflate was well exploited for various synthetic organic transformations.[47] Very recently Rao et al., reported the potential of GaS for the photocatalytic water splitting for the production of H_2.[48] Much remains to be exploited in the realm of the catalytic chemistry of Ga. To gain insights into the reaction pathways of formation of LA from glucose and biomass (cellulose, starch). The possible reaction scheme of production of levulenic acid from the Glucose or cellulose are given in scheme 1.

The presence of Ga@mordenite increased the conversion of either glucose or fructose, especially at 175 °C, and switched the main product from hydroxymethylfurfural to LA (Scheme 1).

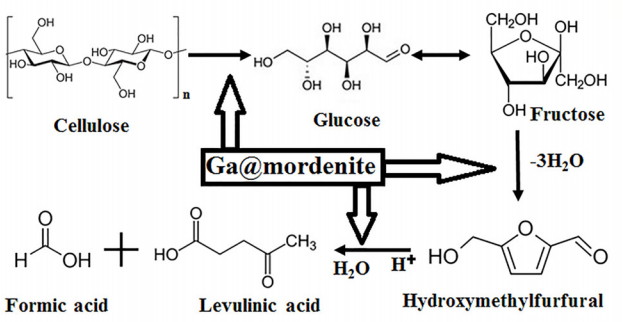

Scheme 1. The possible reaction mechanism for production of levulinic acid (LA) from the cellulose or glucose.

3. Summary and Conclusions

The present works reports a novel sonochemical pathway for the synthesis of Ga modified zeolite (mordenite) catalyst. Use of the novel sonochemical deposition facilitated strong adhesion and homogeneous distribution of small Ga particles throughout the zeolite surface rendering stability to the catalyst. Moreover, use of sonication shortens the duration of the catalyst preparation (2 h) compared to conventional wet impregnation techniques. The solid acid catalyst exhibited good activity for the conversion of glucose, starch and cellulose to levulinic acid. High yields of LA (59.9 wt. %) from glucose under modest reaction conditions (175 °C, 6 h) could be obtained in a hydrothermal process using the Ga@mordenite solid acid catalyst. The reusability of the catalyst was also demonstrated for four consecutive reaction runs. Thus an

environmentally benign catalytic process is developed for the conversion of biomass to an important platform chemical, levulinic acid.

Acknowledgements:

Gedanken thanks the Israel Ministry of Science and Technology for the research grant 3–99763 and the Israel Science Foundation for supporting the research via a grant 598/12. Grateful thanks are due to Dr Pankaj Sharma, The M S University of Baroda, India, for kindly helping us in characterizing Ga@mordenite catalyst with TPD spectrometry.

Keywords: Ga@mordenite · Glucose · Hydrolysis · Hydrothermal process · Levulinic acid · Zeolite

[1] J. Popp, Z. Lakner, M. Harangi-Rákos, M. Fári, *Renew. Sustain. Energy Rev.* **2014**, *32*, 559.
[2] L. Axelsson, M. Franzén, M. Ostwald, G. Berndes, G. Lakshmi, N. H. Ravindranath, *Biofuels, Bioprod. Biorefining* **2012**, *6*, 246.
[3] P. McKendry, *Bioresour. Technol.* **2002**, *83*, 47.
[4] A. Corma Canos, S. Iborra, A. Velty, *Chem. Rev.* **2007**, *107*, 2411.
[5] A. M. Raspolli Galletti, C. Antonetti, E. Ribechini, M. P. Colombini, N. Nassi o Di Nasso, E. Bonari, *Appl. Energy* **2013**, *102*, 157.
[6] F. M. Geilen, B. Engendahl, A. Harwardt, W. Marquardt, J. Klankermayer, W. Leitner, *Angew. Chemie - Int. Ed.* **2010**, *49*, 5510.
[7] F. Cherubini, *Energy Convers. Manag.* **2010**, *51*, 1412.
[8] V. B. Kumar, I. N. Pulidindi, A. Gedanken, *Renew. Energy* **2015**, *78*, 141.
[9] O. Tzhayik, I. N. Pulidindi, A. Gedanken, *Ind. Eng. Chem. Res.* **2014**, *53*, 13871.
[10] V. B. Kumar, I. N. Pulidindi, A. Gedanken, *RSC Adv.* **2015**, *5*, 11043.
[11] D. Fegyverneki, L. Orha, G. Láng, I. T. Horváth, *Tetrahedron* **2010**, *66*, 1078.
[12] I. T. Horváth, H. Mehdi, V. Fábos, L. Boda, L. T. Mika, *Green Chem.* **2008**, *10*, 238.
[13] B. Perlatti, M. R. Forim, V. G. Zuin, *Chem. Biol. Technol. Agric.* **2014**, *1*, 1.
[14] A. Victor, I. N. Pulidindi, A. Gedanken, *RSC Adv.* **2014**, *4*, 44706.
[15] F. Studt, I. Sharafutdinov, F. Abild-Pedersen, C. F. Elkjær, J. S. Hummelshøj, S. Dahl, I. Chorkendorff, J. K. Nørskov, *Nat. Chem.* **2014**, *6*, 320.
[16] S. Yan, Z. Wu, Q. Xu, J. J. Wang, J. Hong, J. Li, P. Wang, Z. Zou, *J. Mater. Chem. A* **2015**, *3*, 15133.
[17] J. Toyir, P. Ramirez de la Piscina, N. Homs, *Int. J. Hydrogen Energy* **2015**, *0*, 2.
[18] J. P. Stassi, P. D. Zgolicz, V. I. Rodrguez, S. R. De Miguel, O. A. Scelza, *Appl. Catal. A Gen.* **2015**, *497*, 58.
[19] V. B. Kumar, A. Gedanken, Z. Porat, *Ultrason. Sonochem.* **2015**, *26*, 340.
[20] V. B. Kumar, I. Perelshtein, A. Lipovsky, Z. Porat, A. Gedanken, *RSC Adv.* **2015**, *5*, 25533.
[21] V. B. Kumar, A. Gedanken, D. Avnir, Z. Porat, *ChemPhysChem* **2016**, *17*, 162.
[22] V. Choudhary, S. H. Mushrif, C. Ho, A. Anderko, V. Nikolakis, N. S. Marinkovic, A. I. Frenkel, S. I. Sandler, D. G. Vlachos, *J. Am. Chem. Soc.* **2013**, *135*, 3997.
[23] F. Yang, J. Fu, J. Mo, X. Lu, *Energy and Fuels* **2013**, *27*, 6973.
[24] A. I. Serykh, S. P. Kolesnikov, *Phys. Chem. Chem. Phys.* **2011**, *13*, 6892.
[25] S. Altwasser, A. Raichle, Y. Traa, J. Weitkamp, *Chem. Eng. Technol.* **2004**, *27*, 1262.
[26] P. Simoncic, T. Armbruster, *Am. Mineral.* **2004**, *89*, 421.
[27] C. Chang, P. Cen, X. Ma, *Bioresour. Technol.* **2007**, *98*, 1448.
[28] H. Chen, B. Yu, S. Jin, *Bioresour. Technol.* **2011**, *102*, 3568.
[29] L. Peng, L. Lin, J. Zhang, J. Zhuang, B. Zhang, Y. Gong, *Molecules* **2010**, *15*, 5258.
[30] N. Ya'Aini, N. A. S. Amin, S. Endud, *Microporous Mesoporous Mater.* **2013**, *171*, 14.
[31] J. Jow, G. L. Rorrer, M. C. Hawley, D. T. A. Lamport, *Biomass* **1987**, *14*, 185.
[32] D. Wang, B. Ma, B. Wang, C. Zhao, P. Wu, *Chem. Commun.* **2015**, *51*, 15102.
[33] A. Raichle, S. Moser, Y. Traa, M. Hunger, J. Weitkamp, *Catal. Commun.* **2001**, *2*, 23.
[34] R. Fricke, H. Kosslick, G. Lischke, M. Richter, *Chem. Rev.* **2000**, *100*, 2303.
[35] W. Zeng, D. Cheng, H. Zhang, F. Chen, X. Zhan, *React. Kinet. Mech. Catal.* **2010**, 377.
[36] N. A. S. Ramli, N. A. S. Amin, *Appl. Catal. B Environ.* **2015**, *163*, 487.
[37] M. A. Mellmer, J. M. R. Gallo, D. Martin Alonso, J. A. Dumesic, *ACS Catal.* **2015**, *5*, 3354.
[38] B. Chamnankid, C. Ratanatawanate, K. Faungnawakij, *Chem. Eng. J.* **2014**, *258*, 341.
[39] V. B. Kumar, Y. Koltypin, A. Gedanken, Z. Porat, *J. Mater. Chem. A* **2014**, *2*, 1309.
[40] V. B. Kumar, A. Gedanken, G. Kimmel, Z. Porat, *Ultrason. Sonochem.* **2014**, *21*, 1166.
[41] J. C. V. Kresge, J. S. B. C. T. Kresge, M. E. Leonowicz, W. J. Roth, *Nature* **1992**, *359*, 710.
[42] K. S. Kumar, V. B. Kumar, P. Paik, *J. Nanoparticles* **2013**, *2013*, 1.
[43] K. M. Minachev, V. I. Garanin, V. V. Kharlamov, T. A. Isakova, E. E. Senderov, *Russ Chem Bull* **1969**, *18*, 1611. doi:10.1007/BF00906391
[44] S. Stefanidis, K. Kalogiannis, E. F. Iliopoulou, A. A. Lappas, J. Martínez Triguero, M. T. Navarro, A. Chica, F. Rey, *Green Chem.* **2013**, *15*, 1647.
[45] C. Zhai, D. Summer, C. Rangger, H. Haas, R. Haubner, C. Decristoforo, *J. Label. Compd. Radiopharm.* **2015**, *58*, 209.
[46] A. Ogawa, H. Fujimoto, *Inorg. Chem.* **2002**, *41*, 4888.
[47] G. K. S. Prakash, T. Mathew, G. A. Olah, *Acc. Chem. Res.* **2012**, *45*, 565.
[48] S. Kouser, A. Thannikoth, U. Gupta, U. V. Waghmare, C. N. R. Rao, *Small* **2015**, *11*, 4723.

Submitted: October 16, 2016
Accepted: November 2, 2016